# Controlled Hierarchical Self-Assembly and Deposition of Nanoscale Photonic Materials**

Tatjana N. Milic, Ning Chi, Dalia G. Yablon,
George W. Flynn, James D. Batteas,* and
Charles Michael Drain*

Nature repeatedly demonstrates exquisite control over the molecular forces that underpin the very existence of life. Inspired by nature, the synthetic introduction of specific molecular interactions to guide the association of matter is an overarching theme in current nanoscale materials and device design.[1] The technological and functional advantages of using nanoscaled or molecular components in a variety of devices has been recognized for decades.[1–5] However, the formation of functioning nanoscaled or molecular electronic devices from nonbiological components began in the 1980s.

The formation of self-organized photogated transistors from porphyrins in lipid bilayers is a key example,[6, 7] but the obvious limitation is the stability of the system. With the remarkable progress in the self-assembly of molecular components into specific arrays and polymers, there are many other recent examples of supramolecular species that are proposed as components of nanoscaled devices.[8–11]

The methodologies used to create devices on the nanometer scale can be roughly categorized as those using lithography ("top down") or self-assembly ("bottom up") approaches, with each having advantages and limitations. Certainly, self-assembly is claimed to be an important avenue toward the manufacture of the next generation of nanoscaled molecular materials, especially for use in photonic devices.[2, 7–11] But, there are several critical factors to be considered. Since the vast majority of molecular self-assembly processes are carried out in solution and utilize relatively weak intermolecular forces, can the desired products be reliably deposited onto surfaces and still retain their intended structure and function? Since the components of the self-

assembled structures are organic or coordination compounds, how stable are they electrochemically, thermally, and to dioxygen? If self-assembled entities are to be used in large-scale applications, an important, yet often unacknowledged requirement is that highly pure molecular components or building blocks must be readily synthesized on large scales in high yields. Herein we report the self-assembly of porphyrinic arrays and clusters that address these issues.

Specifically, we demonstrate hierarchical solution-phase organization of self-assembled nonameric porphyrin arrays into columnar stacks that are about 6.2 nm in diameter and 0.4 nm to about 10 nm tall. These heights correspond to stacks of 1 to about 22 nonamers, and represent the self-organization of 21 to about 460 particles, respectively, of four different chemical types. The size of the aggregates is predetermined by the choice of appended alkyl group, solvent, temperature, porphyrin metalation, and an understanding of the secondary organization kinetics. Moreover, these materials can be deposited onto a variety of surfaces with high structural fidelity, with the choice of surface chemistry affording an additional modality for size selection. AFM and UV/Vis analysis shows that once deposited on surfaces these structures are stable in air for more than a year at room temperature, and retain their photophysical properties. Herein we present data for the hierarchical self-assembly of the free-base porphyrins, and note that zinc porphyrin nonameric arrays exhibit similar organizational properties. This approach provides access to a wide variety of closed arrays, and defined structures. Other approaches include liquid crystalline, and polymeric porphyrin materials on surfaces,[12–14] and other networks.[15, 16]

Earlier, we reported the self-assembly and characterization of a 21-component square-planar porphyrin nonamer.[17] The predefined geometry of either the metallo or free-base porphyrins as well as the coordination geometry of the metal-ion linker—all in the correct stoichiometry—dictates the final structure of the self-assembled arrays. In the case of the nonamer, the 180° (*trans*) coordination geometry of the $12 PdCl_2$ species combines with four "L-shaped" porphyrins (**3**) that serve as the corners, four "T-shaped" porphyrins (**2**) that constitute the sides, and one "+-shaped" porphyrin (**1**) which resides in the center (Figure 1). We have since found that the porphyrins may be metalated in situ—during the self-assembly process—by the addition of nine equivalents of one of several acetate salts of the first-row transition metals to the mixture of nine porphyrins and $12 [PdCl_2Bn_2]$. This process represents the self-assembly of a 30 component system. The metalloporphyrin nonamers, where all the porphyrins ligate the same transition metal ($Fe^{II}$, $Co^{II}$, $Ni^{II}$, or $Zn^{II}$) were characterized by the methods used previously.[17]

UV/Vis studies on a series of porphyrin arrays and tapes self-assembled by the same $[PdCl_2Bn_2]$ species[17, 18] reveal a remarkable similarity in the formation kinetics under the same conditions of concentration, solvent, and temperature. The rate of formation of the much more complex 21-particle nonameric array is only slightly slower than the formation of the simple 3-particle dimer or 8-particle tetramer- all occurring in less than 90 seconds (Table 1). This process is an exquisite demonstration of the cooperative formation of

[*] Prof. Dr. C. M. Drain, T. N. Milic
Department of Chemistry and Biochemistry
Hunter College and Graduate Center of
The City University of New York
695 Park Avenue, New York, NY 10021 (USA)
Fax: (+1)212-772-5332
E-mail: cdrain@hunter.cuny.edu

Prof. Dr. J. D. Batteas, Dr. N. Chi
Department of Chemistry
The College of Staten Island and Graduate Center of
The City University of New York
2800 Victory Blvd., Staten Island, NY 10314 (USA)
Fax: (+1)718-982-3910
E-mail: batteas@postbox.csi.cuny.edu

D. G. Yablon, Prof. Dr. G. W. Flynn
Department of Chemistry, Columbia University
3000 Broadway, MC 3167, New York, NY 10027 (USA)

Supporting information for this article is available on the WWW under http://www.angewandte.org or from the author.

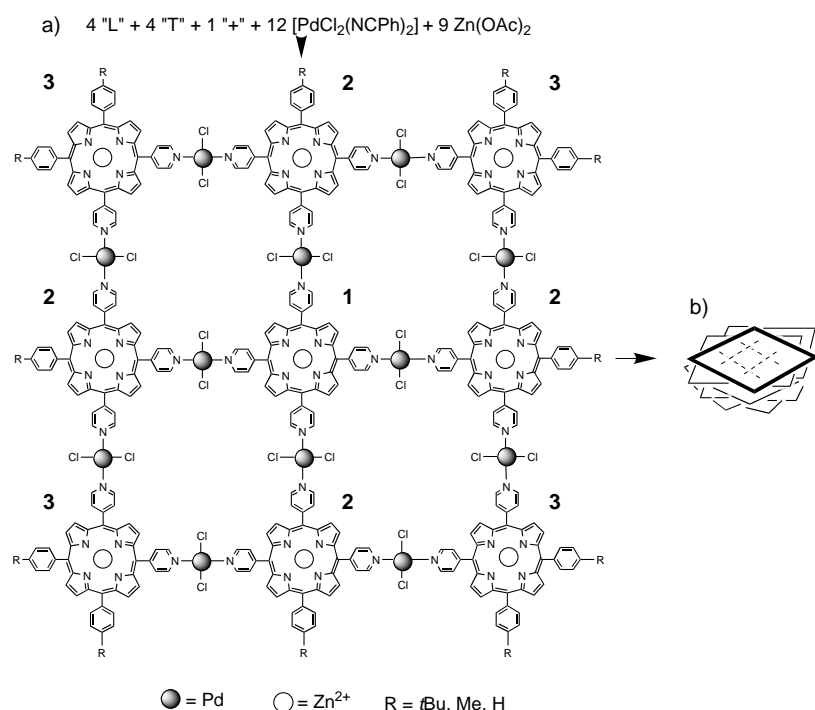a)   4 "L" + 4 "T" + 1 "+" + 12 [PdCl$_2$(NCPh)$_2$] + 9 Zn(OAc)$_2$



b)

Figure 1. a) The self-assembly of a porphyrin nonameric array consisting of 30 particles is followed by b) the self-organization of these nonamers into columnar aggregates that are about 6 nm in diameter and an average of 5 nm in height. The size of these latter entities can be directed by various means (see text).

Table 1. Formation kinetics of porphyrin arrays.

|          | T1 [min] | T2 [min] |
|----------|----------|----------|
| nonamer  | 1.4      | 26       |
| tetramer | 1.2      | 23       |
| dimer    | 0.9      | 14       |

thermodynamic products. The UV/Vis spectral evolution for the arrays continues, revealing a second time constant on the order of about 25 min for the nonamer. Dynamic and resonance light scattering (DLS, RLS), coupled with AFM experiments, reveal that this process is a secondary organization of these discrete self-assembled arrays into nanoscaled aggregates.

A single nonamer array when R = $t$Bu should be about $6.2 \times 6.2$ nm from $t$Bu to $t$Bu and about 0.4 nm in thickness. DLS of aggregates in solution and AFM of aggregates on glass show that the final aggregate is about $6 \pm 1$ nm in diameter and 2–10 nm tall. However, these experiments also suggest that the aggregation process is dynamic, proceeding through several intermediate stages. The initially formed kinetic products are about 30 nm tall aggregates, and these then dissociate and reorganize until the about 6 nm tall average thermodynamic products are formed. Once removed from the equilibrating solution by deposition on glass surfaces and evaporation of the solvent, the particles are trapped in the state of aggregation at the time. This procedure affords a time-based selection of the average particle size to be deposited on surfaces (Figure 2). UV/Vis and fluorescence spectra indicate the about 6 nm tall aggregates of all four types of nonamer (R = Me or $t$Bu, and M = Zn$^{2+}$ or 2 H$^+$) are thermally stable in

toluene in air up to about 80 °C. After cooling to 20 °C, the DLS data on these samples are identical to those before heating.

The energetics of the self-organization of the columnar stacks of porphyrin nonamers arises from the complex interplay between a variety of intermolecular forces. The π stacking of porphyrins to form face-to-face (H) or edge-to-edge (J) aggregates is a well known and understood phenomena.[19] Electronic spectra indicate both types of arrangements are present in the columnar aggregates.[17] Under the conditions described herein however, neither solutions of individual porphyrins or a mixture of them, nor the palladium complex, results in any discernible aggregation as shown by absorption and emission spectra, DLS, or AFM. Estimates of π-stacking interactions are between 3 and 5 kcal mol$^{-1}$ per porphyrin face for meso-tetraphenylporphyrin.[19] Since the aryl groups are not coplanar with the porphyrin, these substituents also sterically prevent exact alignment of the two macrocycles. A second internonamer interaction comes from the PdCl$_2$ groups. The electrostatic and steric interactions arising from the Pd$^{2+}$ and the
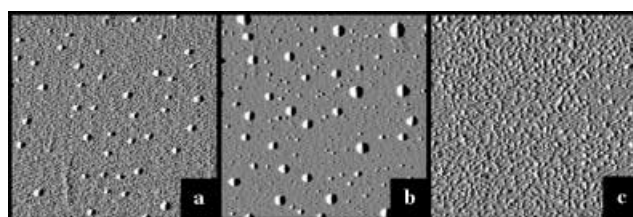


Figure 2. Aliquots of the toluene solution used in the DLS experiments were taken and deposited by syringe onto glass cover slips and the solvent evaporated. After rinsing the samples with toluene, AFM images (10 μm × 10 μm images are light shaded to enhance contrast) were taken to confirm the hypothesis that the formation of the nanoscaled aggregates of free-base porphyrin nonamers (R = Me) is dynamic. a) After 5 min, about 30-nm-high aggregates are first observed, followed by the observation b) of a bimodal distribution of these and 100s of much smaller sub-10-nm-high aggregates, and c) finally a uniform distribution of aggregates that are about 6 nm in height on average. (Since the typical size of the AFM tip was 30–50 nm, all sizes referred to by AFM are the nonamer stack heights, as the horizontal dimensions are a convolution of the tip and aggregate sizes). The AFM results correspond remarkably well with the DLS results.

Cl$^-$ ions would tend to place the Cl$^-$ ions from one nonamer over the vacant axial positions of the Pd$^{2+}$ ions of the adjacent nonamer, over the pyrrole N–H group or in the case of the metalloporphyrins over the zinc(II) center. The nature of R (hydrogen, methyl, or $tert$-butyl), also influences the kinetics and size of the hierarchical assembly. In general, the kinetics are faster and the resultant columnar stacks are larger as one goes from R = $t$Bu, to Me, to H, with average columnar heights, determined by DLS, of 6 nm, 7 nm, 10 nm, respectively. Though the exact geometry of the nanoscaled aggregates is still under investigation, docking experiments suggest

that one planar array may stack on top of another in either of two ways: a) one is rotated 30–60° relative to the next or b) one is diagonally offset by a little more than half the diameter of a single porphyrin about 0.6 nm.

The size of the hierarchical stack formed on the surface may also be explained in terms of the influence of surface energetics on π stacking (Figure 3). AFM studies reveal that
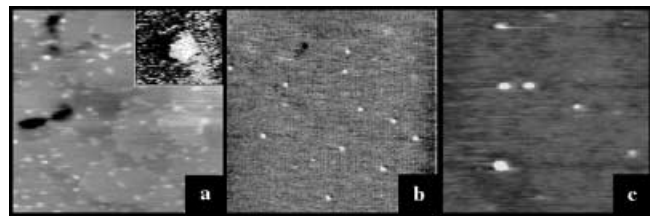


Figure 3. The size of the columnar stack of free-base porphyrin nonamers (R = tBu) is also determined by the nature of the surface. a) Single nonameric arrays are typically found on Au(111) surfaces (the insert shows a single nonamer observed by STM), whereas larger aggregates are observed on b) mica (≈ 5–8-nonamer-high stacks) and c) glass (≈ 5–27-nonamer-high stacks). The images also show the expected increase in the surface density of the nonamers as the aggregates proceed from large stacks on glass to predominantly individual nonamers on Au. All images correspond to 1.15 μm × 1.15 μm, with $z$ scales of 14.2 nm (a), 3 nm (b), and 11.9 nm (c). The insert in panel (a) corresponds to 16 nm × 14 nm with a $z$ scale of about 5 Å, and was collected in constant current mode.

glass and mica surfaces favor absorption of nonamer aggregates, while surfaces such as gold favor dislodging the nonamer in contact with the surface from its parent nanoscaled aggregate and resulting in high surface densities of individual planar nonameric arrays on the gold surface.[20, 21] Interestingly, when nonamers are adsorbed on thin Au films, multi-supramolecular stacks (2–3 nonamers in height) preferentially decorate defects and step edges, while on the atomically flat terraces we find predominantly individual nonamers. This result is most likely due to the local dipoles formed by the Smoluchowski effect[21] at step edges, pinning the nonamers and adding an additional degree of polarization that favors stacking.[22] STM of nonamers on Au(111) clearly show the individual arrays to be about 6 × 6 × 0.4 nm in size (Figure 3 a inset).

Further studies are aimed at evaluating electron conductance of stacked arrays as a function of the number of nonamers in the stacks, and as a function of light intensity. The detailed photonic properties of these aggregates are also under investigation. The controlled formation of nanocrystals and aggregates of inorganic,[23, 24] organic,[25] and hybrid materials[17, 26, 27] such as those described here, is a key step in the development of nanoscaled devices. The cooperative formation of these hierarchical structures, by using both specific and nonspecific interactions, imparts a high degree of stability and control of size not found in most supramolecular systems (Table 2).[28]

[1] P. Ball, Nature 2001, 409, 413–416.
[2] A. P. Alivisatos, P. F. Barbara, A. W. Castleman, J. Chang, D. A. Dixon, M. L. Klein, G. L. McLendon, J. S. Miller, M. A. Ratner, P. J. Rossky, S. I. Stupp, M. E. Thompson, Adv. Mater. 1998, 10, 1297–1336.
[3] M. A. Fox, Acc. Chem. Res. 1999, 32, 201–207.
[4] Ann. N. Y. Acad. Sci. 1998, 852, 1–21 (Eds.: A. Aviram, M. Ratner).
[5] M. A. Reed, MRS Bull. 2001, 26, 113–120.
[6] C. M. Drain, D. Mauzerall, Biophys. J. 1992, 63, 1556–1563.
[7] C. M. Drain, D. Mauzerall, Bioelectrochem. Bioenerg. 1990, 24, 263–266; C. M. Drain, B. Christensen, D. Mauzerall, Proc. Natl. Acad. Sci. USA 1989, 86, 6959–6962.
[8] J.-M. Lehn, Angew. Chem. 1990, 102, 1347–1362; Angew. Chem. Int. Ed. Engl. 1990, 29, 1304–1319.
[9] J. S. Lindsey, New J. Chem. 1991, 15, 153–180.
[10] P. J. Stang, B. Olenyuk, Acc. Chem. Res. 1997, 30, 502–518.
[11] Structure and Bonding 2000, 96, 149–201 (Ed.: M. Fujita).
[12] D. M. Sarno, B. Jiang, D. Grosfeld, J. O. Afriyie, L. J. Matienzo, W. E. Jones, Jr., Langmuir 2000, 16, 6191–6199.
[13] X. Qiu, C. Wang, Q. Zeng, B. Xu, S. Yin, H. Wang, S. Xu, C. Bai, J. Am. Chem. Soc. 2000, 122, 5550–5556.
[14] C.-Y. Liu, H.-I. Pan, M. A. Fox, A. J. Bard, Science 1993, 261, 897–899.
[15] F. Wurthner, C. Thalacker, A. Sautter, Adv. Mater. 1999, 11, 754–758.
[16] D. G. Kurth, P. Lehmann, M. Schutte, Proc. Natl. Acad. Sci. USA 2000, 97, 5704–5707.
[17] C. M. Drain, F. Nifiatis, A. Vasenko, J. D. Batteas, Angew. Chem. 1998, 110, 2478–2481; Angew. Chem. Int. Ed. 1998, 37, 2344–2347.
[18] C. M. Drain, J.-M. Lehn, Chem. Commun. 1994, 2314–2315.
[19] C. A. Hunter, J. K. M. Sanders, J. Am. Chem. Soc. 1990, 112, 5525–5534, and references therein.
[20] G. S. McCarty, P. S. Weiss, Chem. Rev. 1999, 99, 1983–1990.
[21] R. Smoluchowski, Phys. Rev. Lett. 1941, 60, 661–674.
[22] A. P. H. J. Schenning, F. B. G. Benneker, H. P. M. Geurts, X. Y. Liu, R. J. M. Nolte, J. Am. Chem. Soc. 1996, 118, 8549–8552.
[23] V. F. Puntes, K. M. Krishnan, A. P. Alivisatos, Science 2001, 291, 2115–2117.
[24] J. F. Banfield, S. A. Welch, H. Zhang, T. T. Ebert, R. L. Penn, Science 2000, 289, 751–754.
[25] E. R. Zubarev, M. U. Pralle, E. D. Sone, S. I. Stupp, J. Am. Chem. Soc. 2001, 123, 4105–4106.
[26] J. D. Diaz, G. D. Storrier, S. Bernhard, K. Takada, H. D. Abruña, Langmuir 1999, 15, 7351–7354.
[27] T. A. Jung, R. R. Schlitter, J. K. Gimzewski, Nature 1997, 386, 696–698.
[28] C. M. Drain, J. D. Batteas, G. W. Flynn, T. Milic, N. Chi, D. G. Yablan, H. Sommers, Proc. Natl. Acad. Sci. USA, DOI 10.1073/pnas.0/2521899.

Table 2. Control of hierarchical self-assembly.

|  | Average height [nm] |
| --- | --- |
| chemistry: |  |
| R = H | 10 ± 2 |
| R = Me | 7 ± 1 |
| R = tBu | 6 ± 1 |
| surface: |  |
| glass | 6 ± 2 |
| mica | 3 ± 1 |
| Au(111) | 0.4 (single nonamer) |
| Au(111) edge | 0.8 ± 0.3 |
| kinetics: |  |
| 5 min (R = Me) | 30 ± 5 |
| 10 min | 50 ± 8 |
| 30 min | 6 ± 1 |